Raman scattering study of Ge and Sn compounds with type-I clathrate hydrate crystal structure

G. S. Nolas
R&D Division, Marlow Industries, Inc., 10451 Vista Park Road, Dallas, Texas 75238

C. A. Kendziora
Materials Science and Technology Division, Code 6330, Naval Research Laboratory, Washington, DC 20375

(Received 8 November 1999)

Raman scattering spectra of polycrystalline $Sr_8Ga_{16}Ge_{30}$, $Eu_8Ga_{16}Ge_{30}$, $Cs_8Ga_8Sn_{38}$, and $Cs_8Zn_4Sn_{37}Ge_5$, all with the type-I clathrate crystal structure, were studied at room temperature and 10 K. Several of the Raman-active vibrational modes in these compounds have been identified. The Ge and Sn clathrate spectra are similar, with the vibrational modes of the Sn clathrates shifting to lower frequencies as compared to Ge clathrates. Polarization measurements were used to identify the A_g modes. The lower-frequency mode of the two Raman-active modes corresponding to the ''rattling'' vibrations of the ''guest'' atoms inside the tetrakaidecahedral ''cages'' have been identified in these compounds. This mode is at a frequency that is within the acoustic phonon branch of these compounds. The experimental data are compared to theoretical predictions.

INTRODUCTION

The growing interest in open-structured (zeolitelike) semiconducting compounds for thermoelectric applications is due to their characteristically low thermal conductivities. The host atoms in such materials form weak bonds with atoms residing inside atomic ''cages'' formed by the host atoms, resulting in localized vibrational modes that may couple to the lattice modes and thus resonantly scatter acoustic-mode, heat-carrying phonons. In one class of open-structured compounds, the skutterudite material system, very low thermal conductivities were observed upon filling the voids with lanthanide ions.[1] The smaller and more massive the lanthanide ion, the lower the thermal conductivity. Inelastic neutron scattering[2] and Raman scattering[3] data support this picture.

A class of open-structured compounds that are of growing interest as potential thermoelectric materials are referred to as clathrates because they are isotypic with the clathrate hydrates.[4] The type-I clathrate hydrate crystal structure forms with the $Pm\bar{3}n$ space group. The general formula can be written as $A_8X_8(\mathrm{IV})_{38}$ or $B_8Y_{16}(\mathrm{IV})_{30}$, where A is an alkali metal, B is an alkaline earth, X is a group-II element such as Zn, Y is a group-III element such as Ga, and (IV) is a group-IV element, Si, Ge, or Sn. There is one formula unit (54 atoms) per primitive unit cell. The framework in these compounds is formed by covalent tetrahedrally bonded group-IV atoms comprised of two different polyhedra that are connected to each other by these shared faces, two pentagonal dodecahedra, and six tetrakaidecahedra (12 pentagonal and 2 hexagonal faces) per cubic unit cell (Fig. 1).

Recently it has been shown that the thermal conductivity of these materials is quite low, lower than that of vitreous silica near room temperature.[5–9] In most cases the temperature dependence of these materials is atypical of simple crystalline solids,[5–9] and in some cases is similar to that of amorphous materials.[5–7] The low thermal conductivity measured in these compounds (for clathrate hydrates[10] as well as Si, Ge, and Sn clathrates) is due to the weak guest-host interactions whereby the localized guest vibrations interact strongly with the host acoustic modes. The guest translational vibration (or ''rattling'') frequencies increase as the size difference between guest and host polyhedra decreases as a result of the stronger restoring forces of the guest atom.[6,7] From Rietveld refinements of neutron diffraction and single-crystal x-ray diffraction data, large anisotropic atomic displacement parameters are obtained for the guest atom in the tetrakaidecahedral cage.[8,9,11] This is a clear indication of how oversized the cages in these compounds are as compared to their guests. Due to the low thermal conductivities measured in these compounds, as well as the fact that semiconductors

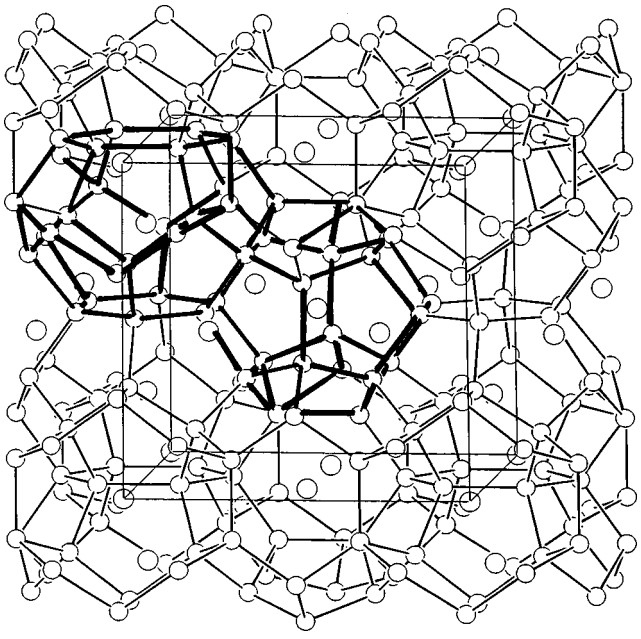

FIG. 1. The type-I clathrate crystal structure highlighting the dodecahedra (20-atom cage outlined at the center of the figure) and the tetrakaidecahedra (24-atom cage outlined at the upper left). The open circles represent atoms forming the (IV_{46}) framework; the guest atoms inside the polyhedra are not shown.

TABLE I. The atomic percentages from electron-beam microprobe analysis, the lattice parameter a_0 in Å, the grain size of densifed polycrystalline samples in μm, measured density D_{meas} in g/cm^3, and x-ray density D_{theory} in g/cm^3 of the four phase-pure polycrystalline specimens.

Compound	Elemental at. %	a_0	Grain size	D_{meas}	D_{theory}
$Sr_8Ga_{16}Ge_{30}$	14.7Sr/29.8Ga/55.5Ge	10.732	17	5.1	5.4
$Eu_8Ga_{16}Ge_{30}$	14.2Eu/28.3Ga/57.6Ge	10.711	5.4	5.4	6.1
$Cs_8Zn_4Sn_{37}Ge_5$	14.7Cs/7.5Zn/69.4Sn/8.4Ge	12.068	7.7	4.8	5.7
$Cs_8Ga_8Sn_{38}$	14.9Rb/14.9Ga/70.2Sn	12.015	14	5.7	5.9

with high Seebeck coefficients and electronic conductivities can be synthesized,[5–7] these compounds are of growing interest for thermoelectric applications. They also continue to be of scientific interest, as indicated by recent high-pressure Raman scattering and NMR measurements on Si clathrates as well as an investigation of the electronic properties of new Si and Ge type-I compounds.[12–14] However, a thorough investigation of the vibrational modes in these interesting compounds has not yet been undertaken.

The vibrational modes of Si clathrate compounds has been investigated experimentally[15,16] and theoretically[17–20] due to their interest as potential superconductor materials. Only recently has a theoretical investigation into Ge clathrates been reported.[21,22] In the present study we investigate the vibrational modes of polycrystalline $Sr_8Ga_{16}Ge_{30}$, $Eu_8Ga_{16}Ge_{30}$, $Cs_8Ga_8Sn_{38}$, and $Cs_8Zn_4Sn_{37}Ge_5$ employing Raman scattering in an effort to begin a systematic survey of the vibrational modes of compounds with this crystal structure. We employ room- and low-temperature (10 K) Stokes and anti-Stokes spectra along with polarization- and excitation-wavelength-dependent measurements. In addition, we investigate the effect of the guest Sr, Eu, or Cs vibrational modes on those of the framework in order to elucidate the effect of the caged atoms on the lattice modes. The experimental results are compared to theoretical predictions.

SAMPLE PREPARATION AND EXPERIMENTAL ARRANGEMENT

The Ge clathrate samples were prepared by mixing and reacting stoichiometric quantities of high-purity constituent elements in a pyrolitic boron nitride (BN) crucible for three days at 960 °C and then annealed at 700 °C for 4 days. The BN crucibles were themselves sealed inside a fused quartz ampoule, which was evacuated and backfilled with argon gas to a pressure of approximately 0.07 MPa. The Ge clathrates were composed of crystals with dimensions of 1–3 mm^3 and were stable in air and water. In the case of the Sn clathrates high-purity elements were mixed in an argon-atmosphere glovebox and reacted for two weeks at 550 °C inside a tungsten crucible, which was itself sealed inside a stainless steel canister. The canister was evacuated and backfilled with high-purity argon gas before sealing. The resulting compounds consisted of small crystallites with a shiny, somewhat blackish, metallic luster. These submillimeter-sized crystals were not very reactive in air or moisture; however, surface oxidation was evident if not stored in a dry box. Powder or single-crystal x-ray diffraction (XRD) was performed on all samples, revealing the crystal structure ($Pm\bar{3}n$) and lattice parameters.

The Ge clathrate (Sn clathrate) specimens were then ground to fine powders and hot pressed inside graphite dies at 700 °C (380 °C) and 170 MPa for 2 h in an argon atmosphere. This resulted in dense pellets which were then cut with a wire saw and polished to a final polish with 0.3 μm alumina paste for the Raman experiments. Electron-beam microprobe analysis of a polished cross section of each specimen revealed the exact stoichiometry of the phase-pure samples. Table I summarizes the chemical and structural data of the four semiconducting clathrate compounds prepared for this work.

The 514.5 nm excitation of an Ar-ion laser and the 647.1 nm excitation of a Kr-ion laser were used in the Raman scattering measurements. The incident beam was backscattered off the sample at a 45° angle to avoid the direct reflection impinging on the collective lens. The collected light was analyzed with a Dilor 500 mm triple-grating spectrometer and counted with a liquid-nitrogen-cooled charge-coupled device array. Due to the low thermal conductivity of the samples, the power incident onto the sample was limited to 75 mW to minimize surface damage. Typical collection times were of the order of 20 min and several scans were averaged to increase the signal-to-noise ratio and remove anomalous spikes. The spectral resolution was 3 cm^{-1} for 514.5 nm excitation and 2 cm^{-1} for 641.7 nm excitation. Low-temperature measurements were made in flowing He vapor to minimize the effects of laser heating.

RESULTS AND DISCUSSION

In the case of $X_8(IV)_{46}$ there are three distinct crystallographic sites in the unit cell of the $Pm\bar{3}n$ crystal structure for the group-IV atoms: $6c$, $16i$, and $24k$ sites. The X guest atoms reside inside two dodecahedra, at the $2a$ crystallographic site, and six tetrakaidecahedra, at the $6d$ site, per unit cell. There are 162 (3×54) Γ-point (**q=0**) phonon modes. From these the first-order Raman-active modes of the $(IV)_{46}$ framework atoms can readily be determined by group theory to be $3A_{2g}+7E_g+8T_{2g}$, where A_{2g} modes are singly degenerate, E_g are doubly degenerate, and T_{2g} are triply degenerate. In addition, the X atom in the $6d$ site also contributes two Raman-active modes ($T_{2g}+E_g$) associated with vibrational modes perpendicular to the sixfold axis (the $2a$ site does not produce Raman-active modes). In the present case we have substituted Ga or Zn for Ge and Sn in order to synthesize semiconducting compounds. Although this should provide specimens with much stronger Raman signals as

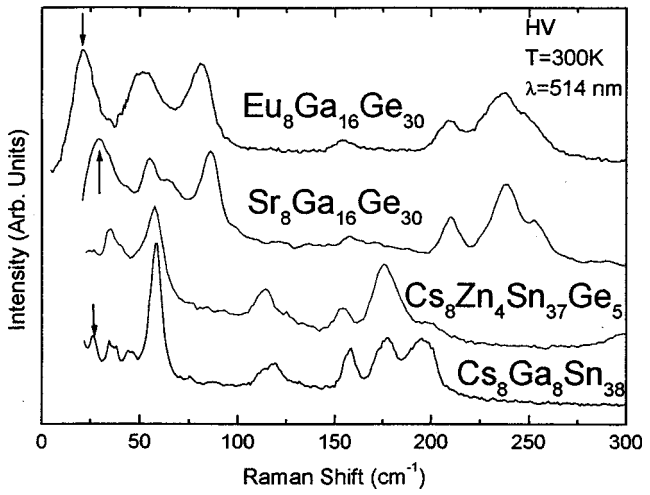

FIG. 2. The Stokes Raman scattering spectra of the four type-I semiconductor clathrates in perpendicular (HV) polarization at room temperature. The arrows represent the vibrational mode associated with the guest Sr or Cs atom inside the tetrakaidecahedra for each specimen.

compared to metallic compounds,[16] it also results in a change of symmetry as compared to $X_8(\mathrm{IV})_{46}$ and therefore more than 20 Raman-active phonon modes are expected. Neutron diffraction measurements[11] on $Sr_8Ga_{16}Ge_{30}$ found the Ga atoms to be randomly distributed on the three Ge sites. We may assume a similar case for $Eu_8Ga_{16}Ge_{30}$. This random distribution of Ga in the Ge framework may decrease the overall symmetry, thereby increasing the total number of Raman-active modes. We take this into account in our analysis, as will be discussed below.

Figure 2 shows room-temperature Stokes Raman spectra up to 300 cm^{-1} for the four specimens prepared for this investigation, using the 514.5 nm Ar^+ laser line. The spectra have been offset on the intensity axis for easy visualization. The incident and collected polarization were perpendicular, generally allowing resolution down to small Raman shifts without a large background from near the Rayleigh line. The spectra consist of relatively sharp and well-defined features. The peak positions and linewidths [full width at half maximum (FWHM)] along with the experimentally determined A_g modes are shown in Table II. In some cases an electronic Raman signal, which appears as a frequency-dependent background, was also observed. The electronic signal was distinguished from photoluminescence by virtue of its independence of incident wavelength, as illustrated in Fig. 3, and by comparing the Stokes and anti-Stokes spectra. Such electronic Raman scattering is not surprising given the relatively large carrier concentration in these compounds.[5,7] Qualitatively similar phenomena are observed in doped semiconductors[3,23] and metals.[24] Some phonon linewidth broadening may result from interaction with this electronic background or may be due to the addition of Ga in the clathrate framework (replacing Ge or Sn) in order to produce semiconducting samples. The FWHM's, however, are narrower than those previously observed in Si clathrates.[15,16] In all four samples the room-temperature spectra have a good signal-to-noise ratio for all observed modes, and we employ these data to fit the spectra and tabulate the Raman lines.

TABLE II. Peak positions, FWHM, and A_g (noted by an asterisk) room-temperature mode assignments of the experimentally observed Raman-active phonon modes for the four polycrystalline type-I semiconductor clathrates. These modes are listed in order of ascending Raman shift, along with their respective FWHM's in parentheses, both in cm^{-1}, with similar mode assignments on the same row.

ν (FWHM)			
$Sr_8Ga_{16}Ge_{30}$	$Eu_8Ga_{16}Ge_{30}$	$Cs_8Ga_8Sn_{38}$	$Cs_8Zn_4Sn_{37}Ge_5$
32(12)	23(10)	26(6)	
56(6)	48(6)	37(4)	33(3)
65(18)	56(14)	47(3)	45(3)
	69(2)		48(10)
86(8)	84(10)	60(6)	59(9)
			73(7)
		116(7)	
126(13)	128(10)		
156(10)	158(13)	121(10)	117(6)
172*(12)	173*(12)	132*(9)	128*(7)
187*(3)	187*(10)	141*(5)	137*(6)
210(10)	211(14)	161(8)	159(7)
		175(5)	175(6)
		181(10)	180(9)
224*(10)	231*(16)		
237(18)	241(19)	196(10)	187(11)
254(9)	256(15)	203(8)	206(11)
		215(2)	

The A_g modes were identified by employing polarization measurements as follows. In general, we may define the depolarization ratio P as $P=I_r/I_p$, where I_p is the Raman scattered intensity polarized parallel to the laser line and I_r is the intensity polarized perpendicular to the laser line.[25] In the case of randomly oriented scattering centers, e.g., polycrystalline specimens, with a cubic crystal structure, $P=0$ for the A_g modes and $P\neq 0$ for all other symmetries. The scattered

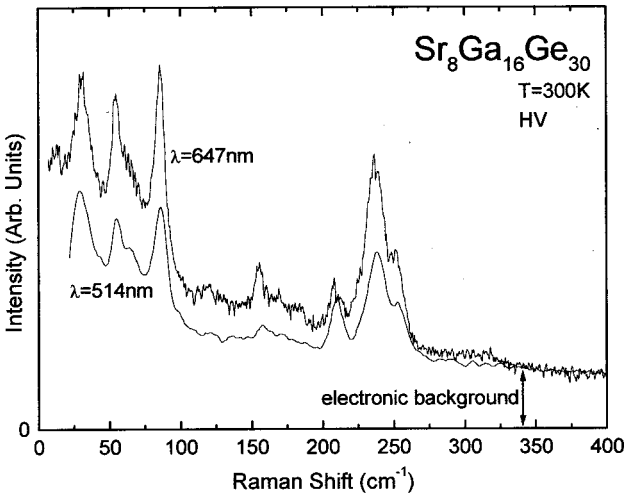

FIG. 3. Stokes Raman scattering spectra of $Sr_8Ga_{16}Ge_{30}$ taken with perpendicular (HV) polarization using 647.1 and 514.5 nm excitation, illustrating the electronic background described in the text.

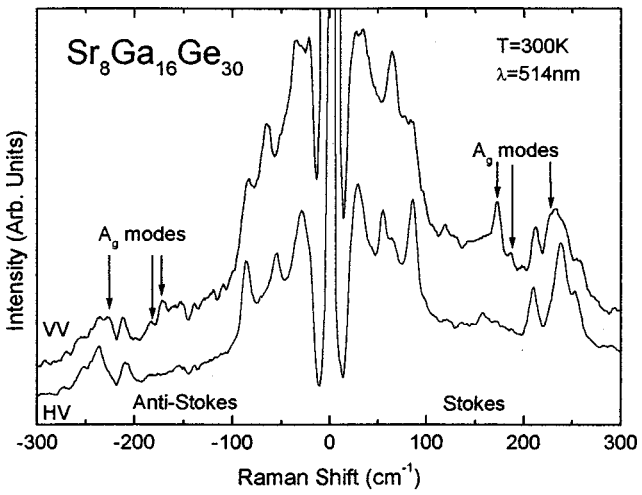

FIG. 4. Stokes and anti-Stokes measurements taken with parallel (VV) and perpendicular (HV) polarization on $Sr_8Ga_{16}Ge_{30}$. Note the difference in intensity of the A_g modes between parallel and perpendicular polarization.

light averages over a large number of scattering centers in a polycrystalline sample where the grain size is much smaller than the incident-beam focus.[25] The degree of depolarization can therefore distinguish the A_g symmetry modes from the other vibrational modes. Figure 4 illustrates this approach with the Stokes and anti-Stokes Raman scattering spectra of $Sr_8Ga_{16}Ge_{30}$ taken with the scattered light polarized parallel (VV) and perpendicular (HV) to the 514.5 nm Ar^+ laser line at room temperature. Contrary to previous measurements on Si clathrates,[15,16] we observe a strong polarization dependence in the A_g modes. These assignments are shown in Table II. We cannot unambiguously identify the other vibrational symmetries, however. In all samples we have used the anti-Stokes spectra to distinguish the Raman signal in these clathrate compounds from artifacts resulting from plasma lines from the laser excitations.

The Raman spectra of $Sr_8Ga_{16}Ge_{30}$ and $Eu_8Ga_{16}Ge_{30}$ are similar to each other (Fig. 2). This indicates that the differences in size and mass between the Sr and Eu guest atoms do not have a great effect on the optical modes, i.e., the $(Ga, Ge)_{46}$ framework modes remain relatively unchanged. All the Raman-active optical modes for these two Ge clathrates lie within the highest optical mode in Ge diamond (304 cm^{-1}). Although the calculated Raman-active mode assignments[22] for the theoretical compound Ge_{46} may not be most appropriate for a direct comparison with our Ge clathrate specimens, in general the theoretically derived spectrum for Ge_{46} is quite similar to that of these two Ge clathrates. In both, three major regions are associated with the Ge type-I clathrate structure: below 100, at ~160, and above 200 cm^{-1}. In our experimental spectra the bands centered at 237 and 241 cm^{-1} for $Sr_8Ga_{16}Ge_{30}$ and $Eu_8Ga_{16}Ge_{30}$, respectively, have a relatively large FWHM as compared to the other Raman-active modes (see Table II). This may indicate partially unresolved modes. These most likely contain more than one Raman mode that are very near one another in frequency. Preliminary results on single-crystal specimens confirm this suspicion. A careful investigation on oriented single-crystal specimens is currently under consideration. All of the experimentally determined vibrational modes associated with the $(Ga, Ge)_{46}$ framework lie above ~ 50 cm^{-1}. This is also the case for Ge_{46}.[22]

As seen in Fig. 2 the spectrum for $Cs_8Ga_8Sn_{38}$ is similar to those of the two Ge clathrates with the optical modes shifted to lower frequencies. This shift is likely due to the atomic weight of Sn being much larger than that of Ge. In addition, $Cs_8Zn_4Sn_{37}Ge_5$ is also quite similar to the Ge clathrates as well as to $Cs_8Ga_8Sn_{38}$. Although Zn is preferentially located on the 6*c* crystallographic site in these compounds,[8] Ge is presumed to be randomly distributed in the three distinct framework sites in $Cs_8Zn_4Sn_{37}Ge_5$. In the case of the $Cs_8Ga_8Sn_{38}$ compound, Ga is preferentially on the 6*c* site, from XRD results; however, the Ga atoms are also randomly distributed in the other two framework sites. A random distribution of the Ga and (Ge+Zn) atoms in these two Sn clathrate compounds therefore results. This is corroborated by the fact that these two compounds have similar Raman spectra. The vibrational modes of these two clathrates are therefore similar to those of the Ge clathrates, as can be seen from the spectra in Fig. 2.

In three of the specimens the lowest Raman-active vibrational mode is assigned to a weak optical vibrational mode of the guest atom inside the tetrakaidecahedral cage, that is, along the direction perpendicular to the axis that connects the two parallel hexagons in the tetrakaidecahedra (see Fig. 1). Recent theoretical calculations[26] indicate the weak and strong (i.e., vibrational mode parallel to the hexagons) modes to be at approximately 25 and 55 cm^{-1}, respectively, for Sn in Ge_{46}. The lower-frequency mode agrees well with our observation for $Sr_8Ga_{16}Ge_{30}$. For $Eu_8Ga_{16}Ge_{30}$ this mode is at a lower frequency because Eu is more massive than Sr. By analogy we make a similar assignment in the case of $Cs_8Ga_8Ge_{38}$. This mode is indicated with an arrow for each spectrum in Fig. 2. Recent band-structure calculations[21,22] indicate the acoustic modes to be lower than 60 cm^{-1}, placing this ''rattle'' mode well within the acoustic phonon branch. These optic modes may therefore resonantly scatter the acoustic phonons, as evidenced by the low thermal conductivities measured in these compounds with temperature dependences that are atypical of simple solids.[5–9] This is similar to the case of the clathrate hydrates where the localized low-frequency optic modes of the guest molecules couple to the acoustic phonon branches of the host lattice, thereby resonantly scattering the acoustic phonons.[11,27] The other Raman-active rattle mode associated with the vibrations of the guest in the tetrakaidecahedra may hybridize with the lower-frequency modes associated with the framework atoms. From our spectra this may very well be the case; however, we tentatively assign the $Sr_8Ga_{16}Ge_{30}$ Raman-active mode at 56 cm^{-1} to the framework vibrations.

CONCLUSION

We have investigated and assigned many of the Raman-active optic modes of four semiconducting type-I clathrates: $Sr_8Ga_{16}Ge_{30}$, $Eu_8Ga_{16}Ge_{30}$, $Cs_8Ga_8Sn_{38}$, and

$Cs_8Zn_4Sn_{37}Ge_5$. The vibrational modes associated with the framework atoms range from 48 to 256 cm^{-1} in the case of the Ge clathrates and 37 to 215 cm^{-1} for Sn clathrates. A localized rattle mode with the guest atom inside the tetrakaidecahedra is also identified. This mode is in the range of the acoustic phonons in these compounds. This is in agreement with the band-structure calculations as well as the thermal transport properties associated with these compounds.

ACKNOWLEDGMENT

The authors wish to thank Otto Sankey and Jianjun Dong for very fruitful discussions as well as preliminary calculations on optic modes of ''filled'' type-I Ge clathrates. G.S.N. acknowledges support from the U.S. Army Research Laboratory under Contract No. DAAD17-99-C-0006 and C.A.K. acknowledges support from the Office of Naval Research.

[1] G. S. Nolas, D. T. Morelli, and T. M. Tritt, Annu. Rev. Mater. Sci. **29**, 82 (1999), and references therein.
[2] V. Keppens, D. Mandrus, B. C. Sales, B. C. Chakoumakos, P. Dai, R. Coldea, M. B. Maple, D. A. Gajewski, E. J. Freeman, and S. Bennington, Nature (London) **395**, 876 (1998).
[3] G. S. Nolas and C. A. Kendziora, Phys. Rev. B **59**, 6189 (1999).
[4] See, for example, F. Franks, *Water, A Comprehensive Treatise* (Plenum, New York, 1973).
[5] G. S. Nolas, J. L. Cohn, G. A. Slack, and S. B. Schujman, Appl. Phys. Lett. **73**, 178 (1998).
[6] J. L. Cohn, G. S. Nolas, V. Fessatidis, T. H. Metcalf, and G. A. Slack, Phys. Rev. Lett. **92**, 779 (1999).
[7] G. S. Nolas, in *Thermoelectric Materials—The Next Generation Materials for Small-Scale Refrigeration and Power Generation Applications*, edited by T. M. Tritt, G. Mahan, H. B. Lyon, Jr., and M. G. Kanatzidis, MRS Symposia Proceedings Vol. 545 (Materials Research Society, Pittsburgh, 1999), pp. 435–442.
[8] G. S. Nolas, T. J. R. Weakley, and J. L. Cohn, Chem. Mater. **11**, 2470 (1999).
[9] G. S. Nolas, T. J. R. Weakley, J. L. Cohn, and R. Sharma, Phys. Rev. B **61**, 3845 (2000).
[10] J. S. Tse and M. A. White, J. Phys. Chem. **92**, 5006 (1998).
[11] B. C. Chakoumakos, B. C. Sales, D. G. Mandrus, and G. S. Nolas, J. Alloys Compd. **296**, 80 (1999).
[12] G. K. Ramachandran, P. F. McMillan, J. Diefenbacher, J. Gryko, J. Dong, and O. F. Sankey, Phys. Rev. B **60**, 12 294 (1999).
[13] R. F. Herrmann, K. Tanigaki, T. Kawaguchi, S. Kuroshima, and O. Zhou, Phys. Rev. B **60**, 13 245 (1999).
[14] Y. Guyot, L. Grosvalet, B. Champagnon, E. Reny, C. Cros, and M. Pouchard, Phys. Rev. B **60**, 14 507 (2000).
[15] S. L. Fang, L. Grigorian, P. C. Eklund, G. Dresselhaus, M. S. Dresselhaus, H. Kawaji, and S. Yamanaka, Phys. Rev. B **57**, 7686 (1998).
[16] Y. Guyot, B. Champagnon, E. Reny, C. Cros, M. Pouchard, P. Melinon, A. Perez, and J. Gregora, Phys. Rev. B **57**, R9475 (1998).
[17] M. Menon, E. Richter, and K. R. Subbaswamy, Phys. Rev. B **56**, 12 290 (1997).
[18] D. Kahn and J. P. Lu, Phys. Rev. B **56**, 13 898 (1997).
[19] K. Yoshizawa, T. Kato, M. Tachibana, and T. Yamabe, J. Phys. Chem. A **102**, 10 113 (1998).
[20] J. Dong, O. F. Sankey, and G. Kern, Phys. Rev. B **60**, 950 (1999).
[21] J. Dong, O. F. Sankey, A. A. Demkov, G. K. Ramachandra, J. Gryko, P. McMillan, and W. Windle, in *Thermoelectric Materials—The Next Generation Materials for Small-Scale Refrigeration and Power Generation Applications* (Ref. 7), p. 443.
[22] J. Dong and O. F. Sankey, J. Phys.: Condens. Matter **11**, 6129 (1999).
[23] G. Abstreiter, M. Cardona, and A. Pinczuk, in *Light Scattering in Solids IV*, Vol. 54 of *Topics in Applied Physics*, edited by M. Cardona and G. Guntherodt (Springer-Verlag, Berlin, 1984), pp. 119ff.
[24] A. Zawadowski and M. Cardona, Phys. Rev. B **42**, 10 732 (1990).
[25] See, for example, W. Hayes and R. Loudon, *Scattering of Light by Crystals* (Wiley, New York, 1978).
[26] J. Dong and O. F. Sankey (private communication).
[27] J. S. Tse, V. P. Shpakov, V. V. Murashov, and V. R. Belosludov, J. Chem. Phys. **107**, 9271 (1997).